University of Nebraska - Lincoln

DigitalCommons@University of Nebraska - Lincoln

Mechanical & Materials Engineering Faculty Publications

Mechanical & Materials Engineering, Department of

9-6-2019

3D printing of silk fibroin-based hybrid scaffold treated with platelet rich plasma for bone tissue engineering

Liang Wei
Xi'an Polytechnic University & University of Nebraska Medical Center & Donghua University

Shaohua Wu
University of Nebraska Medical Center & Qingdao University

Mitchell Kuss
University of Nebraska Medical Center

Xiping Jiang
University of Nebraska Medical Center

Runjun Sun
Xi'an Polytechnic University, Xi'an

See next page for additional authors

Follow this and additional works at: https://digitalcommons.unl.edu/mechengfacpub

Part of the Mechanics of Materials Commons, Nanoscience and Nanotechnology Commons, Other Engineering Science and Materials Commons, and the Other Mechanical Engineering Commons

Wei, Liang; Wu, Shaohua; Kuss, Mitchell; Jiang, Xiping; Sun, Runjun; Patrick, Reid; Qin, Xiaohong; and Duan, Bin, "3D printing of silk fibroin-based hybrid scaffold treated with platelet rich plasma for bone tissue engineering" (2019). *Mechanical & Materials Engineering Faculty Publications*. 417.
https://digitalcommons.unl.edu/mechengfacpub/417

Authors

Liang Wei, Shaohua Wu, Mitchell Kuss, Xiping Jiang, Runjun Sun, Reid Patrick, Xiaohong Qin, and Bin Duan

3D printing of silk fibroin-based hybrid scaffold treated with platelet rich plasma for bone tissue engineering

Liang Wei[a,b,c], Shaohua Wu[b,d], Mitchell Kuss[b], Xiping Jiang[b], Runjun Sun[a], Reid Patrick[e], Xiaohong Qin[c,**], Duan Bin[b,f,g,*]

[a] School of Textile Science and Engineering, Xi'an Polytechnic University, Xi'an, 710048, PR China
[b] Mary & Dick Holland Regenerative Medicine Program, Division of Cardiology, Department of Internal Medicine, University of Nebraska Medical Center, Omaha, NE, 68198, USA
[c] Key Laboratory of Textile Science & Technology, Ministry of Education, College of Textiles, Donghua University, Shanghai, 201620, PR China
[d] College of Textiles & Clothing, Qingdao University, Qingdao, 266071, PR China
[e] Department of Pathology & Microbiology, College of Medicine, University of Nebraska Medical Center, Omaha, NE, 68198, USA
[f] Department of Surgery, College of Medicine, University of Nebraska Medical Center, Omaha, NE, 68198, USA
[g] Department of Mechanical and Materials Engineering, University of Nebraska-Lincoln, Lincoln, NE, 68516, USA

ARTICLE INFO

ABSTRACT

3D printing/bioprinting are promising techniques to fabricate scaffolds with well controlled and patient-specific structures and architectures for bone tissue engineering. In this study, we developed a composite bioink consisting of silk fibroin (SF), gelatin (GEL), hyaluronic acid (HA), and tricalcium phosphate (TCP) and 3D bioprinted the silk fibroin-based hybrid scaffolds. The 3D bioprinted scaffolds with dual crosslinking were further treated with human platelet-rich plasma (PRP) to generate PRP coated scaffolds. Live/Dead and MTT assays demonstrated that PRP treatment could obviously promote the cell growth and proliferation of human adipose derived mesenchymal stem cells (HADMSC). In addition, the treatment of PRP did not significantly affect alkaline phosphatase (ALP) activity and expression, but significantly upregulated the gene expression levels of late osteogenic markers. This study demonstrated that the 3D printing of silk fibroin-based hybrid scaffolds, in combination with PRP post-treatment, might be a more efficient strategy to promote osteogenic differentiation of adult stem cells and has significant potential to be used for bone tissue engineering.

1. Introduction

Currently, autologous bone graft is the clinical gold standard treatment for bone repair. The obvious disadvantages of autologous bone graft are their insufficient availability of donor grafts, as well as donor site complications [1]. Tissue engineered grafts provide some attractive insights into practicable approaches for bone tissue repair and are promising substitutes for autologous bone grafts [2].

3D printing techniques have been developed and implemented to generate engineered tissues and organs to facilitate tissue regeneration [3,4]. In addition, they can also be used to fabricate medical devices, such as stents and splints, for clinical use [5,6]. 3D bio-printed scaffolds have many advantages, such as customized and precise architecture, interconnected pore structures, and controllable shapes and sizes [7].

These beneficial properties facilitate potential patient-specific graft fabrication and also promote *in vitro* and *in vivo* cell growth and proliferation [8–10]. Currently, the most commonly-used polymers include hydrogels (e.g. alginate [11], gelatin [12], hyaluronic acid [13]) and polyesters (e.g. polycaprolactone (PCL) [14,15], poly-lactic-co-glycolic acid (PLGA) [16], and polylactic acid (PLA) [17]). More novel and green natural bioink systems are still required for 3D printing application. In addition, apart from biomaterial choices, other bioactive factors also need to be incorporated to promote tissue regeneration.

Silk fibroin (SF) has attracted a great deal of attention in the tissue engineering field over the last 30 years [18]. It exhibits great mechanical properties and biodegradation properties. In addition, SF is nontoxic, nonimmunogenic, and has been approved by the United States Food and Drug Administration to fabricate some medical

products for human applications [19,20]. Moreover, SF has successfully been processed into various types of scaffolds, such as films, nanofibers, gels, and sponges [21–23]. Therefore, SF has been widely used in bone tissue engineering applications [24–27]. In this work, the SF based composite bioink mixture was prepared by adding gelatin (Gel), hyaluronic acid (HA), and beta tricalcium phosphate (β-TCP), and its 3D printability was further explored.

Among various bioactive factors, platelet-rich plasma (PRP) is a therapeutic agent used to promote tissue regeneration [28]. PRP is an autologous concentration of human platelets with a cocktail of growth factors, including platelet-derived growth factors (PDGF-AA, PDGF-BB, and PDGF-AB), transforming growth factors (TGF1 and TGF3), vascular endothelial growth factor (VEGF), and basic fibroblast growth factor (bFGF) [29–31]. In previous reports, PRP treatments have been demonstrated to improve the healing outcome of injured tissues, including tendons and ligaments [32–34]. Recently, some other studies indicated that PRP treatment is instructive to enhance the osteogenic differentiation of adipose-derived stem cells and promote bone regeneration [35,36].

In this study, we aimed to fabricate a novel SF/GEL/HA/TCP based composite scaffold by employing a 3D bioprinting technique. PRP was further isolated and implemented to treat the 3D printed scaffolds. We seeded human adipose derived mesenchymal stromal cells (HADMSC) on the scaffolds with and without PRP treatment and investigated the effects of PRP treatment on the growth, proliferation, and osteogenic differentiation of HADMSC.

2. Materials and methods

2.1. Preparation of aqueous silk fibroin solution

Aqueous SF solution was fabricated according to a previous report [23], with minor changes. To be brief, silk cocoons (Mulberry Farms) were cut into small pieces and further added into boiling water with 0.02 M Na_2CO_3 (Sigma) for 30 min to remove sericin. The degummed SF fibers were washed three times to remove residual Na_2CO_3 and air-dried in the hood for 24 h. The aqueous SF solution was fabricated by dissolving the SF fibers in 9.3 M lithium bromide (LiBr, Alfa Aesar) solution in the oven at 120 °C for 4 h until all the fibers completely dissolved, forming a yellow, transparent solution. This yellow, transparent solution was dialyzed in deionized water using a dialysis bag (Pierce, MWCO 3500). The final concentration of the aqueous SF solution was calculated to be 6.8% (w/v).

2.2. Fabrication of the SF-based composite scaffold by 3D printing

The SF-based composite bioink was prepared by adding GEL (Bovine skin type B, Sigma), HA (~1200 kDa, NovaMatrix), and β-TCP (nanocrystals, Berkeley Advanced Biomaterials) into aqueous SF solution. First, 0.4 g GEL was added into 10 ml 6.8% (w/v) aqueous SF solution and magnetically stirred at 37 °C until the GEL completely dissolved. After that, 0.2 g HA and 1 g β-TCP were added into the SF/GEL solution and stirred continuously at 37 °C for 3 h to generate the SF/GEL/HA/TCP bioink mixture. Before 3D printing, the bioink mixture was placed in a 4 °C atmosphere for 10 min. A 3D Bioplotter (3D-Bioplotter® Manufacturer Series, EnvisionTEC) was used to 3D bioprint the SF/GEL/HA/TCP composite gel bioink, which has a printing axis resolution of 0.001 mm. To create the printed scaffold, the bioink was extruded through a 22-gauge needle (0.413 mm inner diameter) using a pressure of 1.8–2.2 bar and a print head movement speed of 5–8 mm/s. The scaffold was printed as a 20 × 20 mm square with a 3-layer thickness (≈1.25 mm). In this pattern, the layers were printed in an alternating pattern, in which each one was aligned 90° from the layer below it. The obtained scaffolds were placed in 6-well culture plates for further crosslinking. First, 4 ml of 90% (v/v) ethanol was added into each well to crosslink the SF for 10 min. Then the ethanol solution was
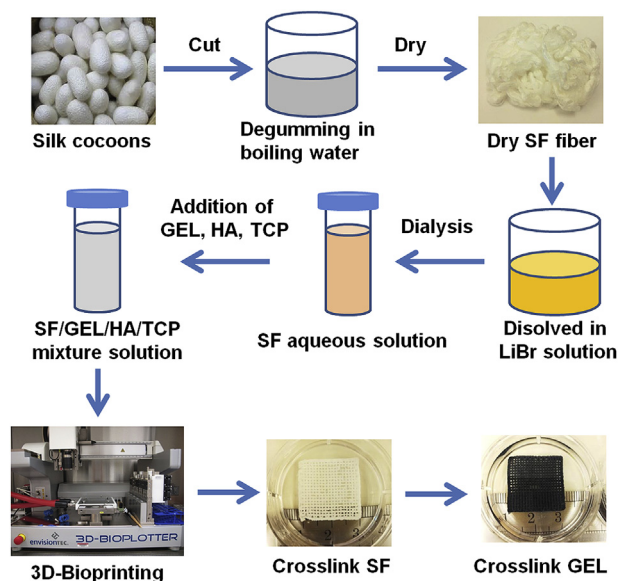

Fig. 1. Schematic illustration of the fabrication of the SF-based hybrid scaffold.

removed, and 4 ml of 0.6% (w/v) genipin (Challenge Bioproducts Co., Ltd.) ethanol solution was added into each well. The well plates were then placed in the 37 °C atmosphere for 72 h to crosslink the gelatin. Thus, a structure-stable SF/GEL/HA/TCP composite scaffold was fabricated. The mechanical properties of the scaffolds were also investigated (Supporting information). The fabrication process is summarized in Fig. 1.

2.3. PRP isolation and elisa analysis for growth factor contents

Human PRP was prepared by sequential centrifugation (Fig. 2 (a)) and was provided by the Elutriation Core Facility at the University of Nebraska Medical Center. PRP was further activated by freeze/thaw cycles, and the released VEGF, bFGF, PDGF-AA, and TGFβ3 were measured using Elisa kits (RayBiotech).

2.4. PRP treatment for SF-based composite scaffolds

PRP post-treatment was employed to modify the composite scaffolds. The composite scaffolds were punched into small discs with a diameter of about 7 mm, sterilized for 2 h using ultraviolet lamp, and
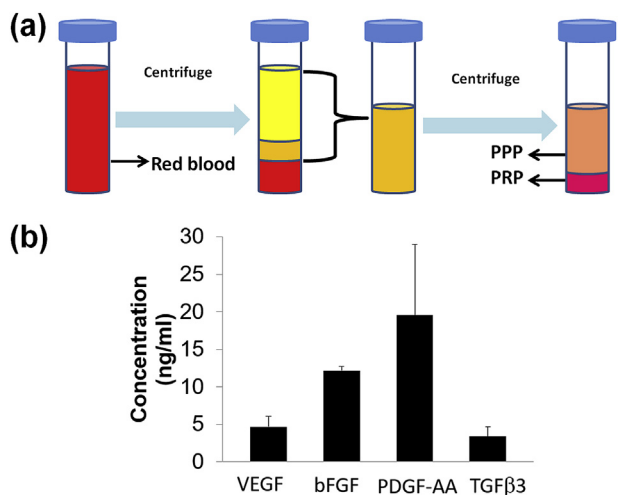

Fig. 2. (a) Schematic diagram of preparation process of PRP, (b) The concentration of different growth factors in PRP (n = 3).

immersed 70% ethanol overnight. These sterilized scaffolds were transformed to place in a 24-well culture plate. Then 500 μl of PRP was added into each well, and the samples were placed in 4 °C overnight. The 3D printed composite scaffolds without PRP treatment were used as control group.

2.5. Surface morphology of SF-based composite scaffolds

The morphologies of two types of composite scaffolds, with and without PRP treatment, were examined by using a scanning electron microscope (SEM, FEI Quanta2000).

2.6. Cell seeding on SF based composite scaffolds

HADMSC (Lonza) were utilized to conduct all cell-related experiments. HADMSC were cultured in growth medium with DMEM/F12 (Life Technologies), 10% fetal bovine serum (FBS, Sigma Aldrich), and 1% penicillin/streptomycin (P/S, GE Healthcare Life Sciences). Before cell seeding, the scaffolds were sterilized by exposure to an ultraviolet lamp for 2 h and immersion in 70% ethanol overnight, and then they were washed three times in sterilized PBS. The HADMSC were seeded at a density of 5×10^4 cells per scaffold. For all of the cell culture experiments, cells were cultured in 5% CO_2 at 37 °C, and the medium was replaced every 2 days. For osteogenic differentiation, osteogenic differentiation medium consisting of DMEM/F12 medium, 10% FBS, 1% P/S, 100 nM dexamethasone (Sigma), 10 mM β-glycerophosphate (Sigma), and 50 μM ascorbic acid (Sigma) was used [37].

2.7. Cell viability

The viability of HADMSC seeded on both PRP non-treated and PRP treated composite scaffolds was evaluated by using a Live/Dead assay [38]. A confocal laser scanning microscope (CLSM, LSM 710, Carl Zeiss) was used to obtain fluorescent images. The cell proliferation of HADMSC on the two scaffold groups was examined at days 7 and 14 by using an MTT assay [39].

2.8. Alkaline Phosphatase (ALP) staining and ALP activity assay

ALP staining was carried out by using an ALP leukocyte kit (Sigma Aldrich), according to the manufacturer's instructions. The ALP activity was operated based on our previous report [40].

2.9. RNA isolation and qPCR

Total RNA was extracted from the HADMSC seeded on the two composite scaffold groups at day 14 by using QIA-Shredder and RNeasy mini-kits (QIAgen). Total RNA was synthesized into first strand cDNA by using an iScript cDNA synthesis kit (BioRad Laboratories). Real-time PCR analysis was performed in a StepOnePlus™ Real-Time PCR System (Thermo Scientific) using SsoAdvanced SYBR Green Supermix (Bio-Rad). The cDNA samples were analyzed for the genes of interest and for the housekeeping gene 18S rRNA. The level of expression of each target gene was calculated using the comparative Ct ($2^{-\Delta\Delta Ct}$) method. The primers used were summarized in Table 1.

2.10. Statistical analysis

All quantitative data is expressed as mean ± standard deviation (SD). Pairwise comparisons between groups were conducted using ANOVA with Scheffé post hoc tests in statistical analysis. A value of p < 0.05 was considered statistically significant.

Table 1
Primer sequences for qPCR.

Gene symbol	Genbank ID	Primer sequences (5′→3′)	Product size (bp)
18S	NR_003286	F: GAGAAACGGCTACCACATCC	170
		R: CACCAGACTTGCCCTCCA	
ALP	NM_000478	F: CCACAAGCCCGTGACAGA	127
		R: GGGCGGCAGACTTTGGTT	
Runx2	NM_001024630	F: TACCTGAGCCAGATGACG	145
		R: AAGGCCAGAGGCAGAAGT	
OCN	NM_199173	F: GGCAGCGAGGTAGTGAAGA	148
		R: CCTGAAAGCCGATGTGGT	
OPN	NM_001040058	F: AAATTCTGGGAGGGCTTGG	117
		R: TTCCTTGGTCGGCGTTTG	

3. Results and discussion

3.1. Preparation of PRP

Fig. 2a shows the schematic diagram of the preparation process of PRP. Human whole blood was subjected to two sequential centrifugation steps (i.e. separation and concentration). The first centrifugation separated pellet plasma, leukocytes, and platelets from the erythrocytes. The second centrifugation collected concentrated platelets in a small volume of plasma (designated as PRP). Fig. 2b shows the concentration of various growth factors in PRP after activation. The results showed that PRP contained VEGF, bFGF, PDGF-AA, and TGFβ3. The PDGF-AA exhibited the highest concentration. All of these growth factors are helpful for the growth and proliferation of osteoblasts and MSC during the bone tissue regeneration process.

3.2. Surface morphology of the SF-based composite scaffolds with and without PRP treatment

The morphologies of composite scaffolds with and without PRP treatment were shown in Fig. 3a–d. Some morphological differences between the material surfaces of the two scaffold groups were observed. For the PRP treated composite scaffold, more small pores were found on the scaffold surface. In addition, both of these two scaffolds presented rough surface morphology.

3.3. PRP treated composite scaffold enhanced HADMSC proliferation

A Live/Dead assay was implemented to evaulate HADMSC viability on the SF-based composite scaffolds. As shown in Fig. 4a–b, most of the HADMSC were alive after 14-day culture on the scaffolds with and
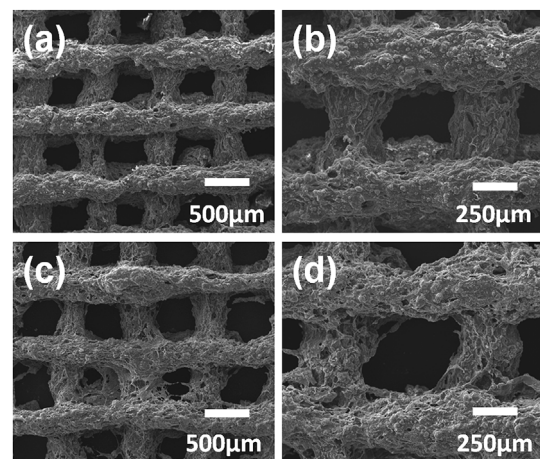

Fig. 3. SEM images of SF-based composite scaffolds: (a, b) composite scaffold without PRP treatment, (c, d) the PRP treated composite scaffold.
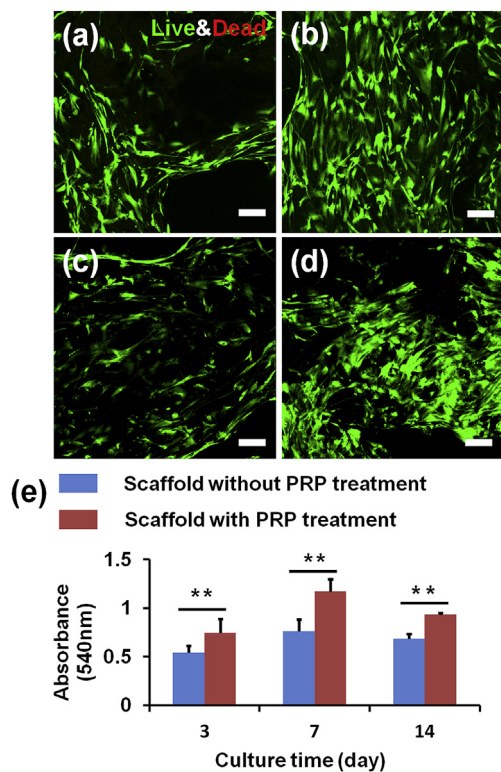
Fig. 4. HADMSC viability and proliferation tests on the SF-based composite scaffolds with and without PRP treatment. Live/Dead images at (7 days, 14 days) of HADMSC seeded on the composite scaffold (a, c) and PRP treated scaffold (b, d). Scale bar: 100 μm. (e) MTT assay for HADMSC proliferation seeded on the two scaffold groups with and without PRP treatment (n = 6; **p < 0.01).

without PRP treatment. The quantitative evaluation of HADMSC proliferation was presented in Fig. 4e. The MTT assay result demonstrated that the cell proliferation rate on the PRP treated composite scaffold was significantly higher than those on the untreated scaffolds from 3 days to 14 days. Several other studies also demonstrated that PRP promoted MSC growth [41,42]. The supportive effects were also dependent on PRP concentration [43] and preparation methods [44]. One of the potential reasons for the benefecial effects of PRP in improving the cell proliferation is that the PRP contained various growth factors, such as VEGF, bFGF, PDGF-AA, and TGFβ3. However, we also found that there was a decreasing trend for the growth speed of HADMSC from 7 days to 14 days. One potential reason was that the growth and proliferation of HADMSC reached confluence on the scaffolds after 14-day culture.

3.4. ALP staining and activity

Fig. 5a and b showed the ALP of staining images of composite scaffolds with and without PRP treatment. After 14 days of osteogenic differentiation, HADMSC were positive to ALP staining on both scaffold groups, but no significant differences were observed between the two different groups. In addition, Fig. 5c showed the ALP activity for the composite scaffolds with and without PRP treatment. The result was in agreement with the ALP staining .

3.5. Gene expression of osteogenic markers of HADMSC cultured on the composite scaffolds with and without PRP treatment

QPCR measurement was employed to compare the osteogenic gene expression level of HADMSC seeded on the two different scaffold groups after 14 days of osteogenic differentiation (Fig. 6). Both early (i.e. ALP
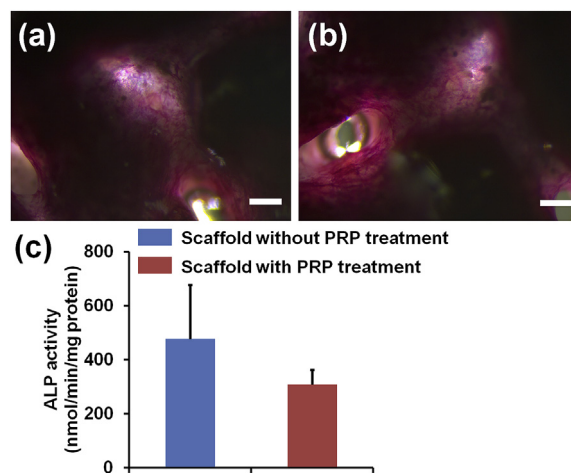

Fig. 5. ALP staining images of the two different SF-based hybrid scaffolds: (a) the pristine SF/GEL/HA/TCP hybrid scaffold, (b) PRP treated SF/GEL/HA/TCP hybrid scaffold, and (c) ALP activity test. Scale bar = 200 μm (n = 6).
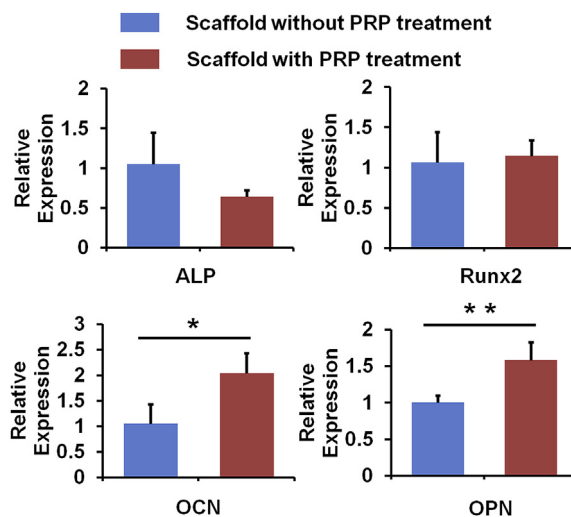

Fig. 6. qPCR analysis of ALP, Runx2, OCN, and OPN genes on HADMSC seeded on the two different SF-based hybrid scaffolds after 14 days culture (n = 6; *p < 0.05, **p < 0.01).

and Runx2) and late (OCN and OPN) stage markers were selected. We found that there was no significant difference in ALP and Runx2 expression, whereas the PRP treatment significantly upregulated the expression of OCN and OPN. Together with previous cell proliferation and ALP staining and activity results, these results indicated that the composite scaffolds with PRP treatment promoted HADMSC proliferation and late osteogenic marker expression. Similarly, Kastern et al. also demonstrated that PRP treatment did not affect ALP activity for bone marrow derived MSC during osteogenic differentiation [45]. One possible reason is probably because the growth factors in PRP do not have long-term effects. This is consistent with our current results. The increase of late stage of osteogenic gene expression is probably due to the higher density of HADMSC, which is the indirect effect of PRP treatment.

4. Conclusions and future perspectives

SF-based composite scaffolds were fabricated by using a 3D printing technique. PRP post-treatment was utilized to modify the 3D-printed composite scaffolds and significantly promoted the HADMSC growth and proliferation, as well as their late-stage gene expression after

osteogenic differentiation. Future efforts should be made to explore strategies to effectively incorporate PRP and control the sustained release of growth factors. In addition, we will further investigate the effects of different PRP concentrations on the HADMSC osteogenic differentiation and the regenerative efficacy after implantation in the bone defect animal models.

Conflict of interest

We declare that we do not have any commercial or associative interest that represents a conflict of interest in connection with the work submitted.

Acknowledgements

Appendix A. Supplementary data

Supplementary data to this article can be found online at https://doi.org/10.1016/j.bioactmat.2019.09.001.

References

[1] M. Braddock, P. Houston, C. Campbell, P. Ashcroft, Born again bone: tissue engineering for bone repair, Physiology 16 (2001) 208–213.

[2] K.K. Tan, G.H. Tan, B.S. Shamsul, K.H. Chua, M.H.A. Ng, B.H.I. Ruszymah, B.S. Aminuddin, M.Y. Loqman, Bone graft substitute using hydroxyapatite scaffold seeded with tissue engineered autologous osteoprogenitor cells in spinal fusion: early result in a sheep model, Med. J. Malays. 60 (Suppl C) (2005) 53–58.

[3] Z. Zhou, F. Buchanan, C. Mitchell, N. Dunne, Printability of calcium phosphate: calcium sulfate powders for the application of tissue engineered bone scaffolds using the 3D printing technique, Mat. Sci. Eng. C-Mater. 38 (2014) 1–10.

[4] S. Pan, Y. Zhong, Y. Shan, X. Liu, Y. Xiao, H. Shi, Selection of the optimum 3D-printed pore and the surface modification techniques for tissue engineering tracheal scaffold in vivo reconstruction, J. Biomed. Mater. Res. A 107 (2019) 360–370.

[5] S.V. Murphy, A. Atala, 3D bioprinting of tissues and organs, Nat. Biotechnol. 32 (2014) 773–785.

[6] D.A. Zopf, S.J. Hollister, M.E. Nelson, R.G. Ohye, G.E. Green, Bioresorbable airway splint created with a three-dimensional printer, N. Engl. J. Med. 368 (2013) 2043–2045.

[7] B. Duan, M. Wang, Selective laser sintering and its application in biomedical engineering, MRS Bull. 36 (2011) 998–1005.

[8] J. Li, M. Chen, X. Wei, Y. Hao, J. Wang, Evaluation of 3D-printed polycaprolactone scaffolds coated with freeze-dried platelet-rich plasma for bone regeneration, Materials 10 (2017).

[9] D.B. Kolesky, R.L. Truby, A.S. Gladman, T.A. Busbee, K.A. Homan, J.A. Lewis, 3D bioprinting of vascularized, heterogeneous cell-laden tissue constructs, Adv. Mater. 26 (2014) 3124–3130.

[10] K. Markstedt, A. Mantas, I. Tournier, H.M. Avila, D. Hagg, P. Gatenholm, 3D bioprinting human chondrocytes with nanocellulose-alginate bioink for cartilage tissue engineering applications, Biomacromolecules 16 (2015) 1489–1496.

[11] S. Naghieh, M.D. Sarker, E. Abelseth, X. Chen, Indirect 3D bioprinting and characterization of alginate scaffolds for potential nerve tissue engineering applications, J. Mech. Behav. Biomed. 93 (2019) 183–193.

[12] J. Lee, C.H. Park, C.S. Kim, Microcylinder-laden gelatin-based bioink engineered for 3D bioprinting, Mater. Lett. 233 (2018) 24–27.

[13] T. Lam, T. Dehne, J.P. Kruger, S. Hondke, M. Endres, A. Thomas, R. Lauster, M. Sittinger, L. Kloke, Photopolymerizable gelatin and hyaluronic acid for stereolithographic 3D bioprinting of tissue-engineered cartilage, J. Biomed. Mater. Res. B (2019), https://doi.org/10.1002/jbm.b.34354.

[14] F. Liu, C. Vyas, G. Poologasundarampillai, I. Pape, S. Hinduja, W. Mirihanage, P. Bartolo, Structural evolution of PCL during melt extrusion 3D printing, Macromol. Mater. Eng. 303 (2018).

[15] S. Bose, S. Vahabzadeh, A. Bandyopadhyay, Bone tissue engineering using 3D printing, Mater. Today 16 (2013) 496–504.

[16] Z. Ge, L. Wang, B.C. Heng, X.-F. Tian, K. Lu, V.T.W. Fan, J.F. Yeo, T. Cao, E. Tan, Proliferation and differentiation of human osteoblasts within 3D printed poly-lactic-co-glycolic acid scaffolds, J. Biomater. Appl. 23 (2009) 533–547.

[17] R.A. Giordano, B.M. Wu, S.W. Borland, L.G. Cima, E.M. Sachs, M.J. Cima, Mechanical properties of dense polylactic acid structures fabricated by three dimensional printing, J. Biomat. Sci-Polym. E. 8 (1996) 63–75.

[18] W. Zhang, L. Chen, J. Chen, L. Wang, X. Gui, J. Ran, G. Xu, H. Zhao, M. Zeng, J. Ji, Wound healing: silk fibroin biomaterial shows safe and effective wound healing in animal models and a randomized controlled clinical trial, Adv. Healthc. Mater. 6 (2017) 1700121.

[19] Z. Zheng, J. Wu, M. Liu, H. Wang, C. Li, M.J. Rodriguez, G. Li, X. Wang, D.L. Kaplan, 3D bioprinting of self-standing silk-based bioink, Adv. Healthc. Mater. 7 (2018) 1701026.

[20] B.B. Mandal, S.C. Kundu, Osteogenic and adipogenic differentiation of rat bone marrow cells on non-mulberry and mulberry silk gland fibroin 3D scaffolds, Biomaterials 30 (2009) 5019–5030.

[21] F. Zhang, X. You, H. Dou, Z. Liu, B. Zuo, X. Zhang, Facile fabrication of robust silk nanofibril films via Direct Dissolution of silk in CaCl2-formic acid solution, ACS Appl. Mater. Interfaces 7 (2015) 3352–3361.

[22] F.G. Omenetto, D.L. Kaplan, New opportunities for an ancient material, Science 329 (2010) 528–531.

[23] D.N. Rockwood, R.C. Preda, T. Yucel, X. Wang, M.L. Lovett, D.L. Kaplan, Materials fabrication from Bombyx mori silk fibroin, Nat. Protoc. 6 (2011) 1612–1631.

[24] J. Qian, A. Suo, X. Jin, W. Xu, M. Xu, Preparation and in vitro characterization of biomorphic silk fibroin scaffolds for bone tissue engineering, J. Biomed. Mater. Res. A 102 (2014) 2961–2971.

[25] J. Melke, S. Midha, S. Ghosh, K. Ito, S. Hofmann, Silk fibroin as biomaterial for bone tissue engineering, Acta Biomater. 31 (2016) 1–16.

[26] H. Xie, Z. Gu, C. Li, C. Franco, J. Wang, L. Li, N. Meredith, Q. Ye, C. Wan, A novel bioceramic scaffold integrating silk fibroin in calcium polyphosphate for bone tissue-engineering, Ceram. Int. 42 (2016) 2386–2392.

[27] S. Pina, R.F. Canadas, G. Jimenez, M. Peran, J.A. Marchal, R.L. Reis, J.M. Oliveira, Biofunctional ionic-Doped calcium phosphates: silk fibroin composites for bone tissue engineering scaffolding, Cells Tissues Organs 204 (2017) 150–163.

[28] W. Zhang, Y. Guo, M. Kuss, W. Shi, A.L. Aldrich, J. Untrauer, T. Kielian, B. Duan, Platelet-rich plasma for the treatment of tissue infection: preparation and clinical evaluation, Tissue Eng. B Rev. (2019) 1–12.

[29] R.E. Marx, Platelet-rich plasma: evidence to support its use, J. Oral Maxillofac. Surg. 62 (2004) 489–496.

[30] R.E. Marx, E.R. Carlson, R.M. Eichstaedt, S.R. Schimmele, J.E. Strauss, K.R. Georgeff, Platelet-rich plasma: growth factor enhancement for bone grafts, Oral Surg, Oral Med.O. 85 (1998) 638–646.

[31] R.E. Marx, Platelet-rich plasma (PRP): what is PRP and what is not PRP? Implant Dent. 10 (2001) 225–228.

[32] L.V. Schnabel, H.O. Mohammed, B.J. Miller, W.G. McDermott, M.S. Jacobson, K.S. Santangelo, L.A. Fortier, Platelet rich plasma (PRP) enhances anabolic gene expression patterns in flexor digitorum superficialis tendons, J. Orthop. Res. 25 (2007) 230–240.

[33] M.M. Murray, K.P. Spindler, E. Abreu, J.A. Muller, A. Nedder, M. Kelly, J. Frino, D. Zurakowski, M. Valenza, B.D. Snyder, S.A. Connolly, Collagen-platelet rich plasma hydrogel enhances primary repair of the porcine anterior cruciate ligament, J. Orthop. Res. 25 (2007) 81–91.

[34] J. Zhang, J.H.C. Wang, PRP treatment effects on degenerative tendinopathy - an in vitro model study, M. L.T.J. 4 (2014) 10–17.

[35] M. Kazem-Arki, M. Kabiri, I. Rad, N.H. Roodbari, H. Hosseinpoor, S. Mirzaei, K. Parivar, H. Hanaee-Ahvaz, Enhancement of osteogenic differentiation of adipose-derived stem cells by PRP modified nanofibrous scaffold, Cytotechnology 70 (2018) 1487–1498.

[36] S. Tajima, M. Tobita, H. Mizuno, Bone regeneration with a combination of adipose-derived stem cells and platelet-rich plasma, Methods Mol. Biol. 1773 (2018) 261–272.

[37] S. Wu, B. Duan, X. Qin, J.T. Butcher, Living nano-micro fibrous woven fabric/hydrogel composite scaffolds for heart valve engineering, Acta Biomater. 51 (2017) 89–100.

[38] S. Wu, B. Duan, P. Liu, C. Zhang, X. Qin, J.T. Butcher, Fabrication of aligned nanofiber polymer yarn networks for anisotropic soft tissue scaffolds, ACS Appl. Mater. Interfaces 8 (2016) 16950–16960.

[39] S. Wu, H. Peng, X. Li, P.N. Streubel, Y. Liu, B. Duan, Effect of scaffold morphology and cell co-culture on tenogenic differentiation of HADMSC on centrifugal melt electrospun poly (L-lactic acid) fibrous meshes, Biofabrication 9 (2017) 044106.

[40] M.A. Kuss, S. Wu, Y. Wang, J.B. Untrauer, W. Li, J.Y. Lim, B. Duan, Prevascularization of 3D printed bone scaffolds by bioactive hydrogels and cell co-culture, J. Biomed. Mater. Res. B. 106 (2018) 1788–1798.

[41] J. Duan, W. Kuang, J. Tan, H. Li, Y. Zhang, K. Hirotaka, K. Tadashi, Differential effects of platelet rich plasma and washed platelets on the proliferation of mouse MSC cells, Mol. Biol. Rep. 38 (2011) 2485–2490.

[42] P.R. Amable, M.V. Telles Teixeira, R.B. Vieira Carias, J.M. Granjeiro, R. Borojevic, Mesenchymal stromal cell proliferation, gene expression and protein production in human platelet-rich plasma-supplemented media, PLoS One 9 (2014).

[43] K. Wang, Z. Li, J. Li, W. Liao, Y. Qin, N. Zhang, X. Huo, N. Mao, H. Zhu, Optimization of the platelet-rich plasma concentration for mesenchymal stem cell applications, Tissue Eng. A 25 (2019) 333–351.

[44] E. Rubio-Azpeitia, I. Andia, Partnership between platelet-rich plasma and mesenchymal stem cells: in vitro experience, M. L.T. J. 4 (2014) 52–62.

[45] P. Kasten, J. Vogel, R. Luginbuhl, P. Niemeyer, S. Weiss, S. Schneider, M. Kramer, A. Leo, W. Richter, Influence of platelet-rich plasma on osteogenic differentiation of mesenchymal stem cells and ectopic bone formation in calcium phosphate ceramics, Cells Tissues Organs 183 (2006) 68–79.